Large area Terahertz digitated photoconductive antennas based on a single high resistivity metal and nanoplasmonic electrode

Anna de Vetter, Chao Song, Martin Mičica, Jérôme Tignon, Juliette Mangeney, José Palomo, Sukhdeep Dhillon

Photonics and Nanostructures - Fundamentals and Applications 59 (2024) 101248

Contents lists available at ScienceDirect

Photonics and Nanostructures - Fundamentals and Applications

journal homepage: www.elsevier.com/locate/photonics

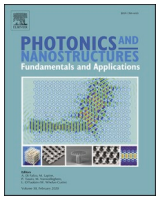

Large area Terahertz digitated photoconductive antennas based on a single high resistivity metal and nanoplasmonic electrode

Anna De Vetter *, Chao Song, Martin Mičica, Jerome Tignon, Juliette Mangeney, José Palomo, Sukhdeep Dhillon *

Laboratoire de Physique de l'Ecole Normale Supérieure (LPENS), ENS, Université PSL, CNRS, Sorbonne Université, Université Paris Cité, Paris 75005, France

ARTICLE INFO

Keywords:
Terahertz
Photoconductive antennas
Time-Domain Spectroscopy

ABSTRACT

Optical excited photoconductive antennas are a central technology for the Terahertz (THz) domain, crucial for both emitting and detecting THz radiation. This work proposes and experimentally realises a new approach in digitated photoconductive antennas (d-PCAs) based on a single digitated high resistivity metal contact with integrated resistances as voltage dividers. This permits a uniform applied electric field over a large surface area and a single step device processing procedure, simplifying the device realisation. This concept is further combined with digitated plasmonic nano-antennas that permits to enhance the light-matter interaction. Through femtosecond optical excitation of such structures, THz pulses can be generated efficiently through this device. Further, for the plasmonic d-PCA, the detected THz electric field of the device shows the effect of polarisation of the incident IR beam, highlighting the role of the nanostructured digitated contacts. This work is supported by electromagnetic simulations showing the optical and THz response of this new type of photoconductive antenna with integrated resistances.

1. Introduction

The terahertz (THz) field of electromagnetic waves offer unprecedented opportunities for a wide array of applications such as spectroscopy, security imaging, medical sensing or ultrafast communications [1]. A particular important technology for the THz range are optically excited photoconductive antennas (PCA). They are typically employed to generate and/or detect broadband THz pulses for time domain spectroscopy (TDS, covering the frequency range from ~ 0.1–4 THz, when excited with a femtosecond laser [2,3]. These antennas exploit the ultrafast photoconductive properties of a semiconductor material to convert ultrafast optical pulses into short THz pulses. The principle is based, in the simplest case, of an applied electric field between two metallic contacts separated by a gap on top of the semiconductor (e.g GaAs). Exciting the material between the gap generates carriers that results in an ultrafast current pulse that radiates as an electromagnetic pulse in the THz range. THz PCAs come in a range of diverse designs, each tailored to specific applications and performance requirements. This includes for example bow tie, parallel line, or logarithmic spiral antennas [2]. These typically, however, have small active gaps (a few microns), meaning that hemispherical silicon lenses need to be integrated to collect efficiently the THz emission. Although large gaps (> 100 μm) can be used, this results in a non-uniform applied electric field with the field stronger at one of the contacts. One prevalent design that overcomes some of these limitations involves large surface area interdigitated electrodes that permits small gaps between electrodes distributed over a large surface area, and a uniform applied electric field between electrodes [4,5], and can be engineered for functionalities such as THz polarisation control [6,7], diffraction limited spectroscopy[8] or coupled to THz cavities[9,10]. However, the process of Interdigitated PCAs requires multiple processing steps where electrodes on deposited of the semiconductor laser, a thick isolating layer of SiO_2 and then a second metallic layer that is composed of metallic fingers covering gaps with a periodicity double that of the first such that the applied electric field is in the same direction. Here we demonstrate a new PCA geometry based using a single contact, high resistivity metal to realise large surface area digitated fingers with integrated resistors to act as voltage dividers and hence a uniform applied field. Further, we show that this single contact geometry can be easily adapted for the incorporation of nanometric plasmonic structures that permits a stronger light-matter interaction and a higher THz field generation.

* Corresponding authors.
E-mail addresses: anna.de-vetter@phys.ens.fr (A. De Vetter), sukhdeep.dhillon@phys.ens.fr (S. Dhillon).

https://doi.org/10.1016/j.photonics.2024.101248
Received 4 December 2023; Received in revised form 28 February 2024; Accepted 29 February 2024
Available online 2 March 2024

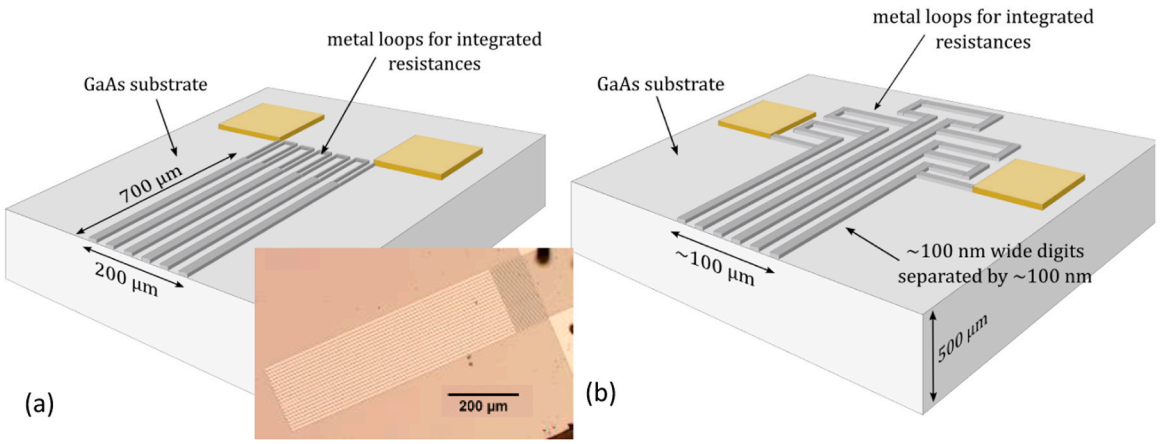

Fig. 1. Schematic of d-PCAs (a). Scheme of d-PCA: single metal 8-µm wide digitated electrode of β-Tantalum were deposited on a 500µm-thick GaAs substrate. The 20 electrodes fingers were spaced by 1.5 µm metal loops that act as integrated resistors. Inset shows the realised device using photolithography (b). Scheme of the nano-structured d-PCA for optical plasmonic confinement: 100 nm-wide digits of Titanium were deposited on a 500µm-thick GaAs substrate. The digits were separated by ~100 nm with Ti metal loops as integrated resistors (not to scale).

2. Design

Here we propose and realise a digitated photoconductive antenna (d-PCA) source that incorporates a single layer grating structure over a large surface area made of high-resistivity metal – β-Tantalum (β-Ta) - with integrated resistors made from the same material. By using the high-resistivity β-Ta, we demonstrate the relatively homogeneous distribution of applied bias over the whole photoconductor resulting in the efficient emission of THz radiation from the d-PCA. Fig. 1(a) shows the schematic of the d-PCA with β-Ta electrodes and whist (b) shows the microscope image of the prototype of the antenna using standard photolithography on semi-insulating GaAs with the Ta deposited at room temperature to ensure the β phase is realised. Here the electrode fingers are 700 µm long over a 200 µm width, with the total of 20 electrode fingers, each 8 µm wide and a spacing of 1.5 µm. The narrow β-Ta metallic loops (2.5 µm wide, 100 µm long) act a resistors and hence as voltage dividers. The digitated electrode is deposited on the surface of 500 µm thick semi-insulated (SI) GaAs substrate. The electrode material β-Ta has a relatively high electrical resistivity $\rho_{\beta\text{-Ta}}$ = 180–220 µΩ·cm [11] in contrast to the gold's electrical resistivity ρ_{Au} = 2.2 µΩ·cm [12] at room temperature. The resistance R of the β-Ta metallic loops then can be determined as R=ρ L/S where ρ represents the electrical resistivity of the material, S and L represent the cross-sectional area and length of the conductor, respectively. We utilized an array of 2.5 µm

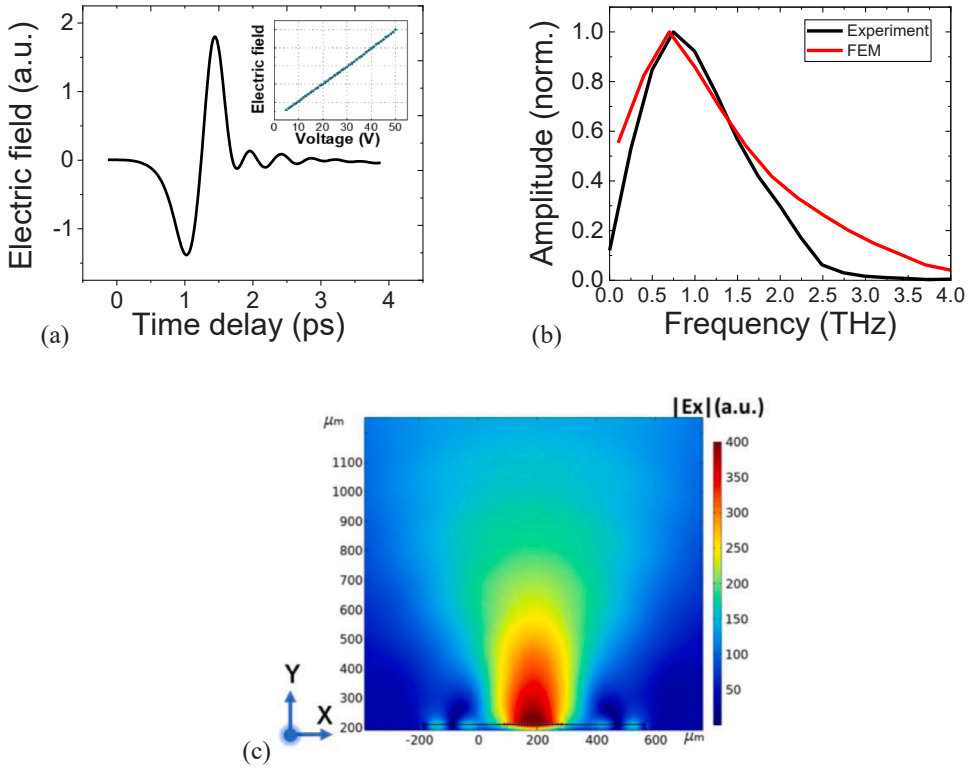

Fig. 2. (a) Time-resolved THz pulse generated by the d-PCA. (b) Peak-to-peak field as a function of applied voltage showing a linear behaviour. (c) Frequency spectrum corresponding to the FT of the time resolved electric field (black line). Red points corresponds to calculated electromagnetic response. (c) Electromagnetic simulations of emitted field from d-PCA at 0.7 THz.

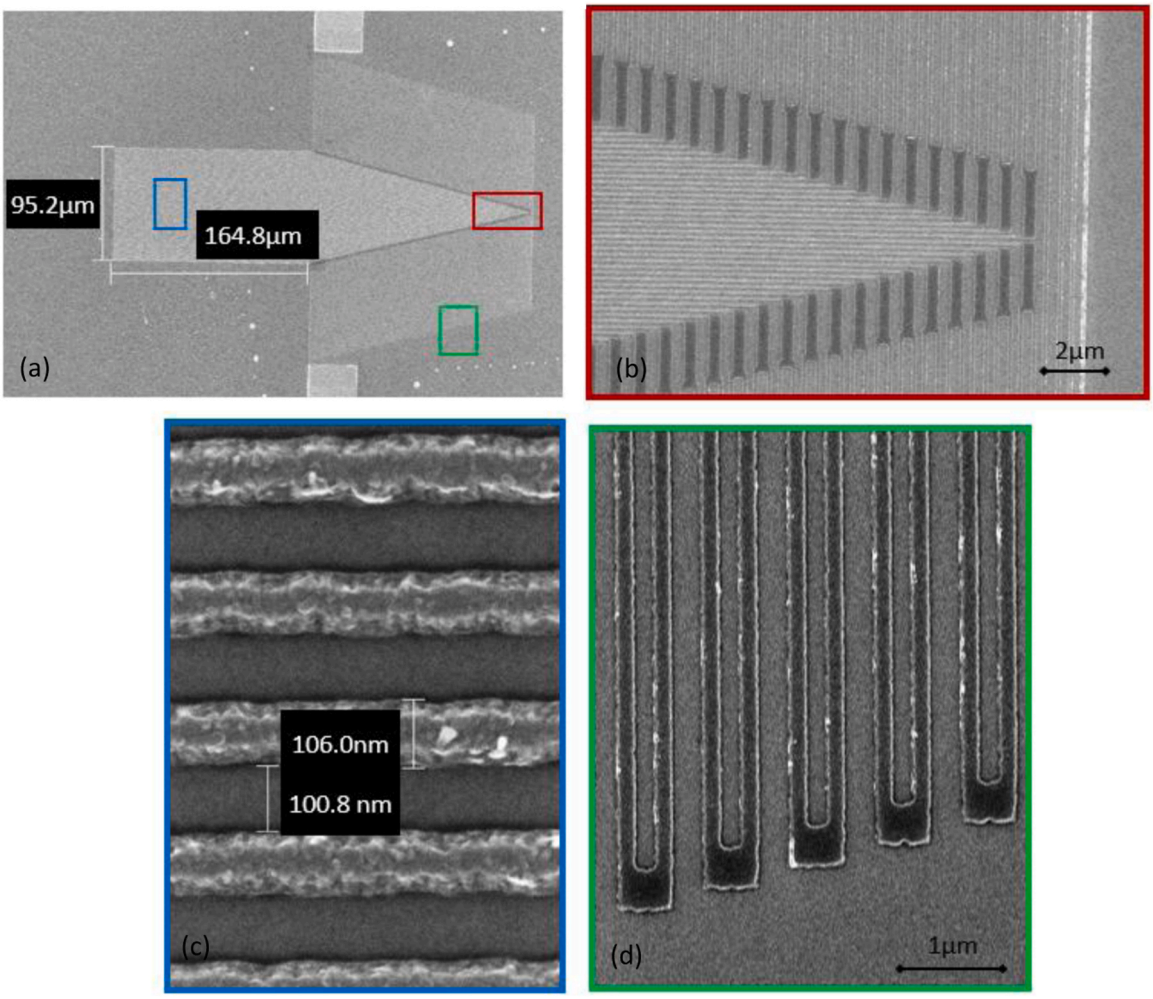

Fig. 3. TEM images of the nanostructured plasmonic d-PCA. (a) Overall design of plasmonic d-PCA with active surface of 165 µm × 95µm. (b) Integrated resistances are implemented on the edges of the digits (red zone) (c) Active area for THz generation showing electrode digits with gaps of 100 nm (blue zone) and (d) shows an enhanced view of the resistance loops (green zone).

narrow, 100 µm long β-Ta electrode fingers as resistors connected in series to act as voltage dividers for the thicker electrode fingers, where due to the longer width (larger cross-section) and consequently lower resistance, electric potential is distributed relatively uniformly over the whole length. A resistance of ~ 400Ω is estimated. The DC field is constant along the length of the digit as confirmed with COMSOL simulations. A nanostructures plasmonic d-PCA is shown in Fig. 1b and is discussed further below.

3. Characterisation

The samples of Fig. 1a were measured in a standard THz-TDS system based on a Ti:Sapphire 100fs oscillator with the d-PCA in reflection geometry. A quasi-static bias field (square wave, 10 Vpp at 80 kHz) is applied to the d-PCA. The PCA was also excited by a femtosecond laser beam with power up to 600 mW and pulse duration ~15 fs. After femtosecond excitation, photo-induced carriers are created by absorption of the pump laser are accelerated, resulting in a time-varying current that radiates as a THz pulse. The emitted THz pulses are collected and focused on to an electro-optic crystal (100 µm thick ZnTe) by series of off-axis parabolic mirrors. The THz electric field waveforms are then measured using standard electro-optic sampling (EO). The whole THz radiation path is purged with dry air to eliminate the absorption of water vapor in the ambient atmosphere. Fig. 2(a) represents the measured time trace of the d-PCA showing a clear single-cycle THz pulse, corresponding to a spectral coverage from a few 100 GHz to ~ 2.5 THz as shown in Fig. 2(b). We further studied the relationship between the bias applied and the detected EO signal up to 50 V (limited by the current pulse generator). The inset of Fig. 2(a) shows a linear dependence of the emitted electric field on applied bias without any saturation effects. Fig. 2(b) also shows the simulated electric field as a function of frequency using COMSOL multiphysics that is modelled as a surface current between the electrode gaps. The emitted field is integrated over probes placed at the top of the d-PCA structure [13] corresponding to the reflection geometry and a good agreement is observed between the simulated and measured fields. (The response of EO crystal is not taken into account as it is relatively flat for the crystal employed in the spectral region investigated). The simulated emission is shown in Fig. 2(c) at 0.7 THz. In terms of emitted THz field strength, this is comparable to interdigitated PCA with equivalent applied fields and surface areas [13].

With the principle experimentally demonstrated and simulated above, we adapted the concept of single metallic contact d-PCA to optical plasmonic gratings (Fig. 1b), highlighting the potential and simplicity of this processing approach. Plasmonic gratings for the optical range refer to periodic structures composed of metallic elements with nanoscale periodicity and exploit the plasmonic properties of metals at optical frequencies to control and manipulate light at the subwavelength scale. The interaction between incident light and localised plasmons of the metallic grating results in a resonance, leading to enhanced electromagnetic fields near the surface [14]. The increased electric field

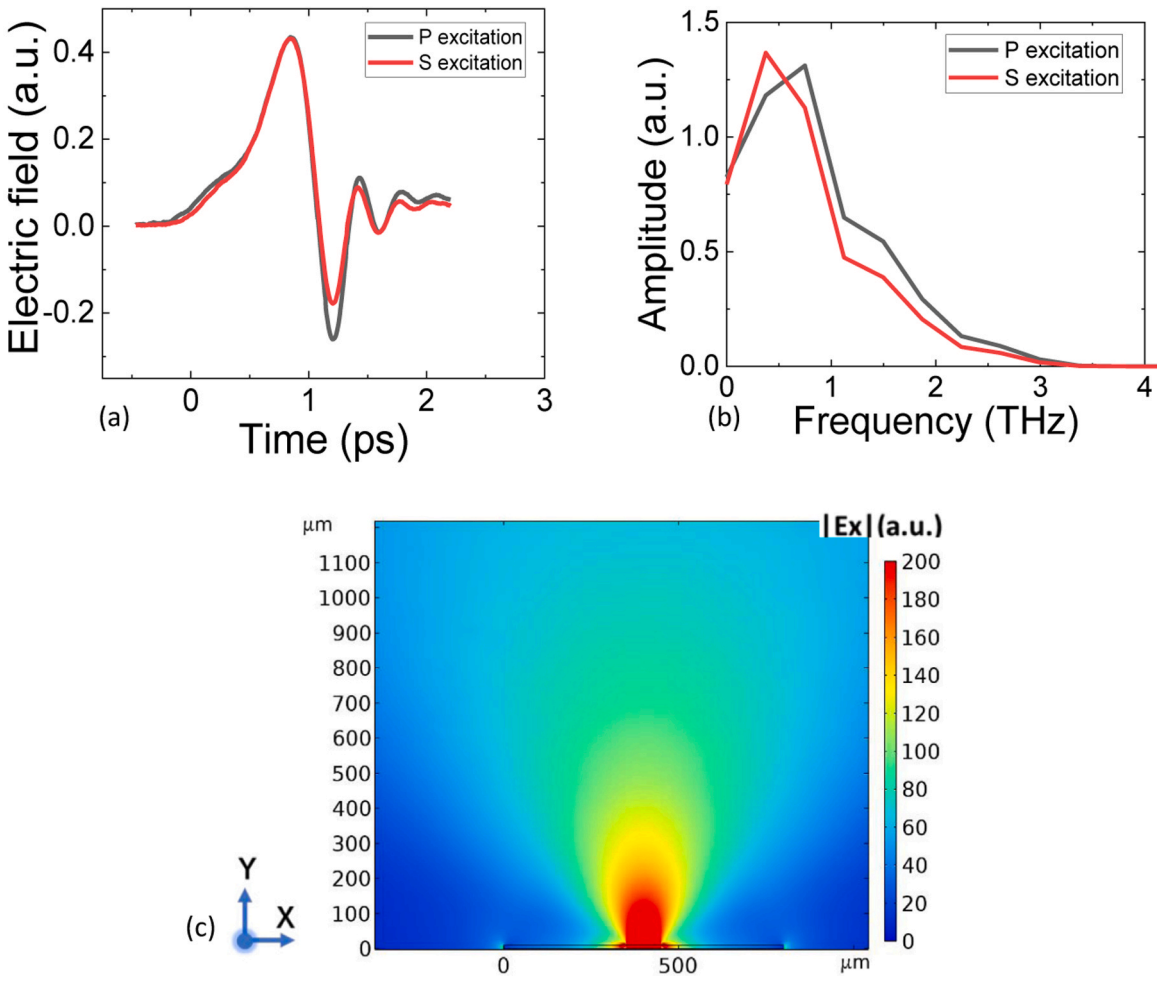

Fig. 4. (a) Non-normalized Time domain THz pulse generated by the plasmonic nano d-PCA and (b) Frequency spectra for the two orthogonal polarization IR excitations (linear y-axis). (c) Electromagnetic simulations of emitted field from nano d-PCA at 0.7 THz.

strength and its strong localization near the nano-scaled object can provide an important increase in absorption in the optical range [15,16]. Plasmonic structures have been applied to interdigitated PCAs [15,17], where one of the electrodes is nanostructured to increase the optical absorption but again requires multiple processing steps.

The schematic of the structure is shown in Fig. 1b and was realized using electron lithography on a 500µm-thick SI GaAs substrate with widths and gaps of 100 nm (Fig. 3a) [15]. The metal used here was Titanium which also has a high resistivity compared to gold, that was further structured in loops to realize integrated resistors (Fig. 3b) perpendicular to the electrode fingers owing to the small dimensions and the number of digits when compared to the simple design of the non-plasmonic structure. Fig. 3b shows the complete device covering a large area of 96µm by 165µm. Although this is smaller than the previous design, leading to a more divergent beam (see below), the concept of this design can be scaled for efficient collection of the THz emission. Regarding processing, e-beam lithography used to define the d-PCA structure and 60 nm-thick Titanium was deposited. For simplicity laser

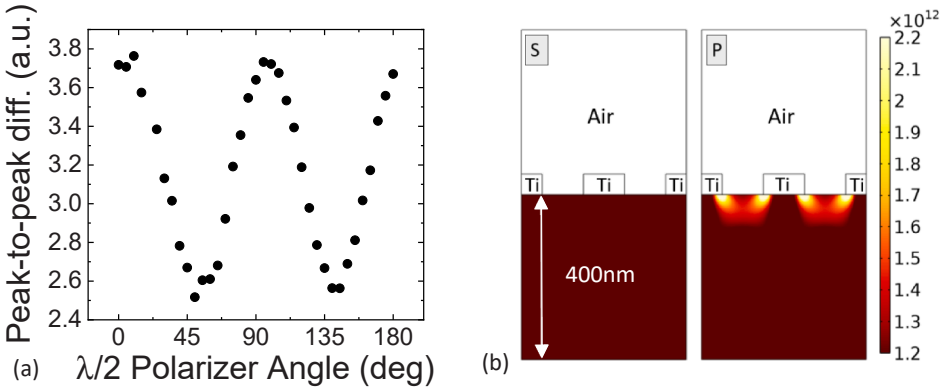

Fig. 5. (a) Influence of the polarization of the IR incident beam on the peak-to-peak signal amplitude of the THz pulse (high frequency oscillations). (b) Total power dissipation density at 800 nm obtained for the plasmonic digits (100 nm wide digits separated by 100 nm) for S and P incident polarization.

lithography was then used to define the large area bonding pad. Each integrated resistance connected to this antenna has an estimated value of 4000Ω with the electric field between each digit of this device is approximately $E = 2\,kV/cm$ for the voltage applied across the entire structure. (This field is limited by the current pulse generator)

The sample was characterised with a similar THz time domain spectroscopy system described above. Here electro-optic sampling with a 200-μm thick ZnTe crystal was employed. To demonstrate the effect of plasmonic confinement and the nanostructuration of the metal, the polarisation of the optical pump beam was controlled using a half wave plate. As can be seen in Fig. 4a, the nano d-PCA showed THz pulse generation with the P polarised beam excitation showing a higher peak-to-peak field when compared S polarised optical excitation for the rapidly varying oscillation of the THz field. (P (S) polarisation corresponds to the electric field of the optical beam perpendicular (parallel) to the electrode and therefore couples to the plasmon mode). This difference in the rapid oscillating field can be seen in the spectrum (Fig. 4b) where the frequency spectrum is considerably wider for the P optical excitation when compared to the S optical case, limited by the detection crystal. This appears to illustrate that carriers are generated closer to the surface, and hence closer to the electrodes resulting in a broader emission [18]. In further detail, the peak-to-peak signal of the rapidly varying part in the time domain (between 1 ps and 1.5 ps) was investigated as a function of half wave plate angle and is shown in Fig. 5, showing an enhanced signal for the IR beam polarized perpendicular to the electrodes with an increase of 50% in these high field oscillations. (Fig. 4c shows the electromagnetic simulations of the emitted field of the nano d-PCA showing a more divergent beam that of Fig. 2 owing to the smaller overall dimensions of the nano d-PCA).

The nanostructured d-PCA was simulated in COMSOL Multiphysics using the Plasmonic Wire Grating method, with an optical wave at 800 nm incident with an array of the plasmonic electrode. Indeed, as the performance of the grating depends on the polarization of the incident wave, both a transverse electric (TE, S polarised) and a transverse magnetic (TM, P polarised) case are simulated. In our case, the TE wave has the electric field component in the z direction, out of the modelling xy-plane so should not couple to the plasmonic grating. For the TM wave, the incident electric field is specified in the xy-plane and perpendicular to the direction of propagation. As shown in Fig. 5b, the highest optical absorption and photo-carrier generation regions are located just near the metal contacts which is the dielectric-metal interface where the excited surface plasmon waves appear for the P polarised wave, resulting in the enhanced THz emission. Although the difference between the S and P absorption is large in the simulations, the experimental results do not show such a large difference and effect of plasmonic confinement. This is possibly a result of the thick substrate where the optical beam is absorbed over a large depth (~1 μm) and not just close to the contact, or that titanium is not the ideal metal for a strong plasmonic confinement[19]. In this case tantalum has a more favourable complex refractive index. There is also the possibility that the top digitated contact acts as a polariser where the P polarisation has an increase transmission compared to S, although the low frequency parts of the THz spectra are similar. Nonetheless, this plasmonic approach could be more beneficial for thin structures (for example thin layers of LT-GaAs for detection[20] or to investigate 2D materials[21])

4. Conclusion

This work has demonstrated a novel large area THz antenna, a d-PCA, based on using high resistive metal such as β-Ta or Ti, permitting a simple processing procedure to realise large area PCAs with a single digitated contact and uniform applied electric field. The approach was further applied to a nanostructured d-PCA permitting enhancemment of the THz field when coupled to TM polarised light. The structure can be signficantly improved such as optimising the fill factor (active excited surface to metal surface), the metal used for the nanostructured d-PCA for improved plasmonic performance, or to couple to THz cavities that would permit to further enhance the emitted THz pulse. As well as impacting THz sources and detectors, this work could impact the interaction of 2D materials and THz ultrafast photocurrents. Indeed, a uniform field can be applied over a large surface area, with a strong optical absorption in an atomically thin material that would result in large THz photocurrents. This would faciltate the investigation of ultrafast transport mechanisms at THz frequencies.

CRediT authorship contribution statement

Anna De Vetter: Writing – review & editing, Writing – original draft, Validation, Methodology, Investigation, Formal analysis. **Jerome Tignon:** Supervision. **Juliette Mangeney:** Supervision. **Chao Song:** Writing – original draft, Visualization, Investigation, Formal analysis. **Martin Micica:** Writing – original draft, Visualization, Investigation, Formal analysis. **Jose Palomo:** Writing – original draft, Methodology, Investigation, Formal analysis, Conceptualization. **Sukhdeep Dhillon:** Writing – review & editing, Writing – original draft, Supervision, Project administration, Methodology, Funding acquisition.

Declaration of Competing Interest

The authors declare that they have no known competing financial interests or personal relationships that could have appeared to influence the work reported in this paper.

Data Availability

Data will be made available on request.

Acknowledgements

A.D.V., C.S., and M.M. contributed equally to this work. The authors acknowledge funding from European Union's Horizon 2020 research and innovation program under grant agreement No 964735 (FETOPEN EXTREME-IR). The authors acknowledge financial support by the European Union's QuantERA II - QATACOMB Project "Quantum correlations in terahertz QCL combs".

References

[1] A. Leitenstorfer, et al., The 2023 terahertz science and technology roadmap, J. Phys. Appl. Phys. vol. 56 (22) (2023) 223001, https://doi.org/10.1088/1361-6463/acbe4c.
[2] Burford, Nathan & El-Shenawee, Review of terahertz photoconductive antenna technology, p. 010901, 2017.
[3] J. Neu, C.A. Schmuttenmaer, Tutorial: an introduction to terahertz time domain spectroscopy (THz-TDS), J. Appl. Phys. vol. 124 (23) (2018) 231101, https://doi.org/10.1063/1.5047659.
[4] Shyamal Mondal, Nisha Flora Boby Edwin, et Vaisshale Rathinasamy, Interdigitated Photoconductive Antenna for Efficient Terahertz Generation and Detection, in Terahertz Technology, Borwen You et Ja-Yu Lu, Éd., Rijeka: IntechOpen, 2022, p. Ch. 9. doi: 10.5772/intechopen.102379.
[5] A. Dreyhaupt, S. Winnerl, T. Dekorsy, M. Helm, High-intensity terahertz radiation from a microstructured large-area photoconductor, Appl. Phys. Lett. vol. 86 (12) (2005) 121114, https://doi.org/10.1063/1.1891304.
[6] K. Maussang, J. Palomo, J. Mangeney, S.S. Dhillon, J. Tignon, Large-area photoconductive switches as emitters of terahertz pulses with fully electrically controlled linear polarization, Opt. Express vol. 27 (10) (2019) 14784–14797, https://doi.org/10.1364/OE.27.014784.
[7] J. Deveikis, J. Lloyd-Hughes, Multi-pixel photoconductive emitters for the controllable generation of azimuthal and radial terahertz beams, Opt. Express vol. 30 (24) (2022) 43293–43300, https://doi.org/10.1364/OE.473086.
[8] M. Baillergeau, et al., Diffraction-limited ultrabroadband terahertz spectroscopy, Sci. Rep. vol. 6 (1) (2016) 24811, https://doi.org/10.1038/srep24811.
[9] K. Maussang, et al., Monolithic echo-less photoconductive switches as a high-resolution detector for terahertz time-domain spectroscopy, Appl. Phys. Lett. vol. 110 (14) (2017) 141102, https://doi.org/10.1063/1.4979536.
[10] K. Maussang, et al., Echo-less photoconductive antenna sources for high-resolution terahertz time-domain spectroscopy, IEEE Trans. Terahertz Sci. Technol. vol. 6 (1) (2016) 20–25, https://doi.org/10.1109/TTHZ.2015.2504794.

[11] M. Magnuson, G. Greczynski, F. Eriksson, L. Hultman, H. Högberg, Electronic structure of β-Ta films from X-ray photoelectron spectroscopy and first-principles calculations, Appl. Surf. Sci. vol. 470 (2019) 607–612, https://doi.org/10.1016/j.apsusc.2018.11.096.
[12] R.A. Matula, Electrical resistivity of copper, gold, palladium, and silver, J. Phys. Chem. Ref. Data vol. 8 (4) (1979) 1147–1298, https://doi.org/10.1063/1.555614.
[13] J. Hawecker, et al., Cavity-based photoconductive sources for real-time terahertz imaging, Photonics Res. vol. 8 (6) (2020) 858–863, https://doi.org/10.1364/PRJ.388219.
[14] V.G. Kravets, A.V. Kabashin, W.L. Barnes, A.N. Grigorenko, Plasmonic surface lattice resonances: a review of properties and applications, Chem. Rev. *118* (12) (2018) 5912–5951.
[15] Yardimci Nezih, Yang Shang-Hua, Berry Christopher, Jarrahi Mona, High-power terahertz generation using large-area plasmonic photoconductive emitters, Terahertz Sci. Technol. (2015) 223–229.
[16] S. Lepeshov, et al., Boosting terahertz photoconductive antenna performance with optimised plasmonic nanostructures, Sci. Rep. vol. 8 (1) (2018) 6624, https://doi.org/10.1038/s41598-018-25013-7.
[17] C.W. Berry, N. Wang, M.R. Hashemi, M. Unlu, M. Jarrahi, Significant performance enhancement in photoconductive terahertz optoelectronics by incorporating plasmonic contact electrodes, Nat. Commun. vol. 4 (1) (2013) 1622, https://doi.org/10.1038/ncomms2638.
[18] J. Madeo, et al., Frequency tunable terahertz interdigitated photoconductive antennas, Electron. Lett. vol. 46 (9) (2010) 611–613, https://doi.org/10.1049/el.2010.0440.
[19] K.J. Palm, J.B. Murray, T.C. Narayan, J.N. Munday, Dynamic optical properties of metal hydrides, ACS Photonics vol. 5 (11) (nov. 2018) 4677–4686, https://doi.org/10.1021/acsphotonics.8b01243.
[20] C.D. Wood, D. Mistry, L.H. Li, J.E. Cunningham, E.H. Linfield, A.G. Davies, On-chip terahertz spectroscopic techniques for measuring mesoscopic quantum systems, Rev. Sci. Instrum. vol. 84 (8) (2013) 085101, https://doi.org/10.1063/1.4816736.
[21] M. Hemmat, et al., Layer-controlled nonlinear terahertz valleytronics in two-dimensional semimetal and semiconductor PtSe2, InfoMat vol. 5 (11) (2023) e12468, https://doi.org/10.1002/inf2.12468.